High Efficiency SOFC Power Cycles With Indirect Natural Gas Reforming and CO_2 Capture

Stefano Campanari[1]
Energy Department,
Politecnico di Milano,
Via Lambruschini 4,
Milano 20156, Italy
e-mail: stefano.campanari@polimi.it

Matteo Gazzani[2]
Energy Department,
Politecnico di Milano,
Via Lambruschini 4,
Milano 20156, Italy

1 Introduction

The adoption of FCs for power production from natural gas with CO_2 capture has long been studied and developed, mainly driven by the very high theoretical efficiency. The majority of the proposed power cycles solutions relies on high temperature FCs, namely, SOFCs and MCFCs. Indeed, they feature the most reasonable possibilities of being industrialized in the very next decades and remarkable R&D results have been achieved during the last 10–15 years, with rather successful experimentations in terms of performances, availability, and sufficiently low performance degradation.

Concerning the integration of power production and CO_2 capture within natural gas based SOFC, several studies have been performed in the last years, starting with early works in the 1990s and around 2000 [1–5]. The majority of these studies is based on the concept of hybrid FC plus gas turbine cycles, where high temperature FCs are integrated with a simple or modified Brayton cycle.

Depending on the SOFC integration with the natural gas reforming/shift section, two main plant solutions can be identified: (i) systems where natural gas is—partially or totally—internally reformed in the FC [6] and (ii) systems where natural gas is reformed before the FC, which is therefore fed with a high hydrogen syngas [7,8]. Cycle configurations of the first type are the most commonly considered by developers of high efficiency power generation plants based on SOFCs and gas turbines [9–11]. In both cases, CO_2 can be separated downstream the FC with a "post-FC capture" layout, via a range of available technologies, e.g., chemical separation processes [3,12,13], physical separation processes [4,14–16], oxy-combustion [11,17–21], and cryogenic methods [22].

Following the above reported literature review on very promising plant configurations, this work investigates the advantages and limits of adopting an external natural gas conversion section for enhancing the plant efficiency. As a reference plant, we considered a power cycle proposed by Adams and Barton [8], whose performance is the highest found in literature for any type of SOFC-based power cycle, featuring a stunning 82% LHV electrical efficiency. It is based on a prereforming concept, where fuel is reformed ahead the SOFC, which has the advantage of working

[1]Corresponding author.
[2]Present address: Institute of Process Engineering, ETHZ, Sonneggstrasse 3, Zurich 8092, Switzerland.

Contributed by the Advanced Energy Systems Division of ASME for publication in the Journal of Fuel Cell Science and Technology. Manuscript received December 3, 2014; final manuscript received December 14, 2014; published online January 13, 2015.

with a high hydrogen fuel. In order to achieve a high efficiency, the external reformer is thermally integrated with the SOFC: all the heat generated in the SOFC system is ideally assumed to be released at high temperature to drive the reformer and several other preheating loops. This plant was first reproduced consider-ing all the assumptions proposed by the original authors [8] and correctly reproducing its calculated performances. As a second step, the simulations were focused on updating the power cycle, implementing a complete set of assumptions about component losses and technological constraints on their operating conditions, which are discussed in detail. Following the consequent modifications with respect to the original layout, the net electric efficiency remains remarkable but decreases to around 63% LHV with nearly complete (95%+) CO capture. The cycle discussion indeed evidences that the resulting power plant layout is very complex and features an extremely demanding heat exchangers network, while it does not generate useful power from the associ-ated gas turbine cycle, working like a turbocharging system.

2 Cycle Simulation

The proposed power cycle is based on a prereforming concept, where fuel is reformed ahead the SOFC, working with a high hydrogen fuel, aiming to avoid any issue of carbon deposition and thermal stress due to internal reforming. The FC works at about 1000 °C and 10 bar. At the cathode side, air comes from an inter-cooled compressor, and the pressurized cathode exhaust is expanded in an air turbine.

At the FC outlet, residual fuel is burned with oxygen produced in a dedicated air separation unit (ASU); the resulting stream is then used primarily to generate steam for a bottoming cycle and to feed the reformer. It is then sent to compression, separation of water, cooling, and liquefaction of CO_2.

Aiming at achieve a high efficiency, the external reformer is thermally integrated with the SOFC. In order to accomplish this, in the original plant configuration [8], all the heat generated in the SOFC system is ideally assumed to be released at high tempera-ture to drive the reformer and several other preheating loops. Heat is also recovered from shift cooling for the same purposes. In all cases, heat is considered as a stream which can be ideally delivered around the plant, neglecting minimum temperature dif-ferences; ideal assumptions are made for most conventional components.

Based on this approach, the original authors apply the power cycle to a very large scale plant, obtaining an extremely high calculated performance: the power plant works at 73.9% HHV (around 82% LHV) electrical efficiency, producing 815 MW net electricity, most of which is produced by the SOFC stacks, with 100% CO_2 capture. Although these remarkable results come from a number of ideal assumptions—so that they can be considered like an ideal reference—efficiency level is the highest found in literature, making the plant configuration interesting.

2.1 Calculation Tool. The thermodynamic model of the assessed power cycles is carried out with the modular simulation code "GS," a tool developed since early 1990s at the Energy Department of Politecnico di Milano [23]. It has provided highly accurate results in a variety of complex plant configurations, including gas turbine cycles, combined cycles [23,24], coal based power plants [25], and hybrid cycles [26,27]. The code integrates models for the prediction of gas and steam turbines and FC performance [23,27] and has been applied to benchmarking CO_2 capture power plants within specific EU projects [28].

The SOFCs are modeled through a lumped volume approach, which calculates mass and energy balances, in this case with no attempt of predicting the FC voltage or temperature profile. Calculation is based on the assumption of an air oxygen utilization fac-tor (UO_2) and a cell voltage (V_c). At the anode side, the model calculates thermodynamic properties and chemical composition of the outlet stream as a function of inlet composition, temperature, and fuel utilization factor (U_f).

2.2 Cycle Simulation With Original Conditions. The power cycle layout originally proposed by Adam and Barton [8] has been redesigned with our power cycle simulation tool (GS) to investigate its performance. The simulation approach adopted by the original authors, based on Aspen Plus, does not require the development of an actual heat exchange network (i.e., without heat transfer fluid) but relies on the free allocation of heat transfer among all components. On the contrary, our simulation code requires to design an appropriate heat exchangers network. Figure 1 reports the rather complex plant layout resulting from this activity. The arrangement of the heat exchanger network fol-lows the necessity to transfer heat at different temperatures among the cycle components. Given that the temperature of the heat transfer fluid must vary in wide range (about 200–950 °C), for the purpose of simulation, it has been assumed to use an inert and cheap gas as nitrogen. Each colored line in the figure represents one or more than one parallel N_2 streams flowing from one heat exchanger to another one. Details about line interpretation are given in the figure caption.

The first part of the analysis has been dedicated to reproducing the original performances of the power cycle considered as a reference, using the same assumptions proposed by the authors. In order to feed the FC with a high hydrogen content syngas, the natural gas stream has to follow the conventional steps for hydrogen production, i.e., prereforming, reforming, high temperature, and low temperature water gas shift. The thermal integration between the external reformer and the FC allows minimizing the exergy losses caused by an external-fired or an autothermal reformer (usually in the range of 8–10% of the LHV energy input [29]). Extraction of heat from the FC is modeled here dividing the SOFCs in two subsystems (or modules) with lower reactant utili-zation and intermediate cooling. The resulting heat network before the FC is rather complex: first, the natural gas must be heated up to the prereformer and the reformer temperature of 500 and 950 °C, respectively; second, the syngas exiting the reformer must be cooled to meet the shift temperature range (200–350 °C). Finally, the hydrogen rich stream must be heated to the FC work-ing conditions (910 °C). Mass balances and thermodynamic conditions for this configuration are shown in Table 1.

The FC is fed with reactants at 910 °C and generating exhausts at 960 °C. At the anode, it is assumed that 86% of the H_2 stream is consumed within the FCs (fuel is 63% H_2, 20% H_2O, and 16% CO_2), with an ideal cell voltage of 0.96 V. On the air side, the SOFC works with a high oxygen utilization (about 87%), so that the outlet O_2 fraction is higher than 3%.

After the FC, the residual fuel is burned with oxygen produced by the ASU unit, generating a 1400 °C pressurized $H_2O + CO_2$ stream. As done by Adams and Barton [8], the amount of oxygen produced in the ASU corresponds in this first analysis to the stoichiometric value for the exhaust combustion. The heat recovery after the FC is based on different heat exchangers (HE) which cool both the anode and cathode exiting stream. This hot gas from the oxy-combustion is used to generate steam at 550 °C for a steam bottoming cycle and high temperature steam at 950 °C and 12 bar for the reformer plus additional heat for SOFC reactant preheating, exiting a heat exchanger network at 50 °C. As already mentioned, ideal heat exchangers are assumed, neglecting minimum temperature differences and heat losses.

The heat recovery steam cycle is based on a typical configuration for subcritical plant but for the boiler which is substituted with an HRSG. Differently from the traditional HRSG, the hot section is based on a closed, nitrogen-based loop which conveys all the excess heat around the plant.

Given the adopted plant working conditions, the CO_2 concentration at the anode exhaust, after the H_2 oxidation and the water condensation, already satisfies storage standards (purity $> 96\%$),

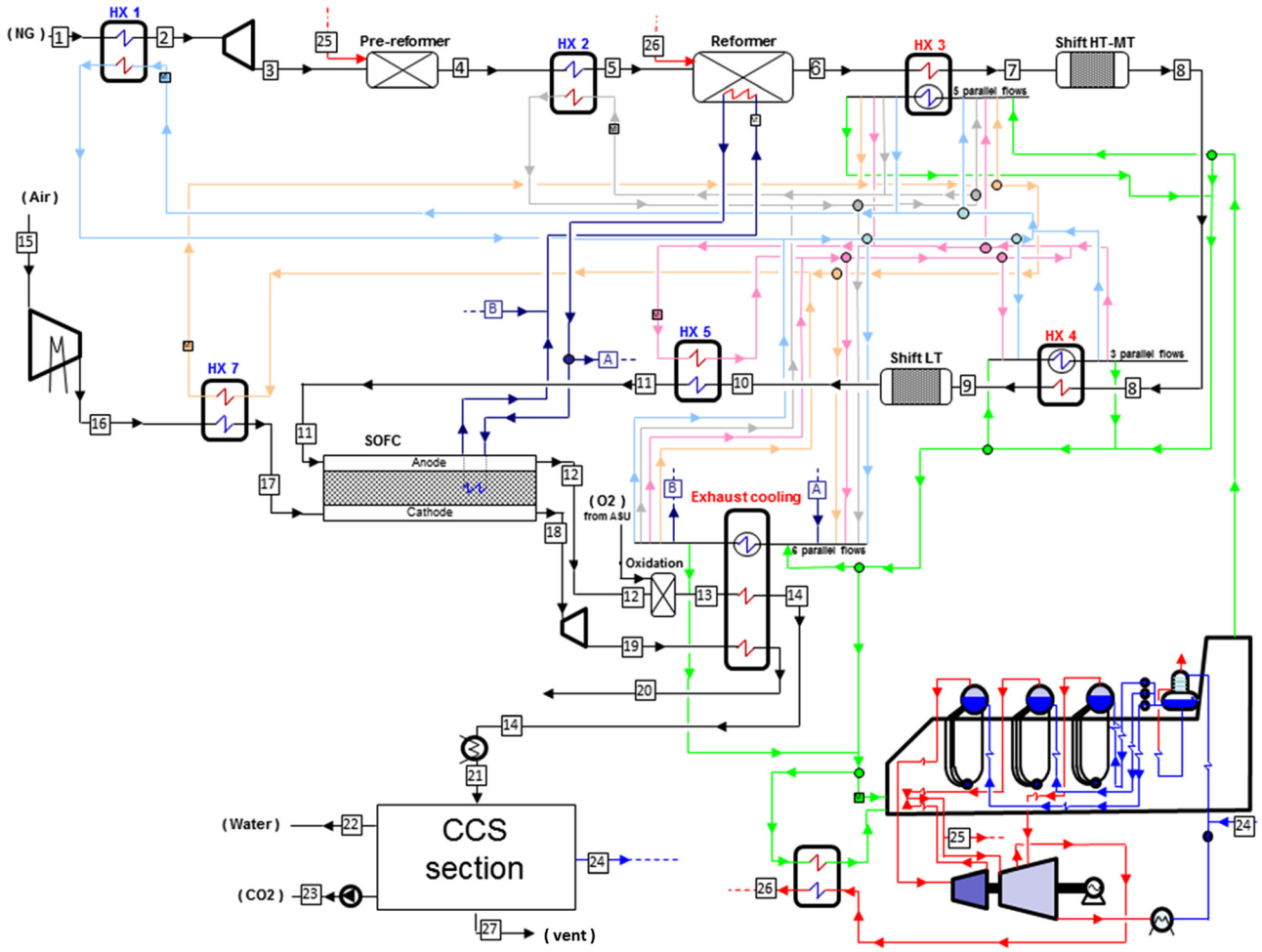

Fig. 1 Plant layout for the investigated SOFC cycle, adapted from its original proposal [8]. Details about the flow arrangement are discussed in the text. For the colored version refer to the digital copy. Blue and red lines around the HRSG section (bottom right in figure) are related to water and steam flows. Each of the other colored line represents one or more than one parallel nitrogen streams, flowing from one to another heat exchanger. Points where a N_2 stream is split from a mainstream are represented with dots. Other crossing of N_2 lines do not indicate a mixing process, which instead occurs ahead heat exchangers in the points represented with squares (this representation is used to avoid drawing too many parallel lines). Some heat exchangers work with a number of parallel flows indicated in the figure and collapsed in a single line for simplicity and compactness of representation.

therefore avoiding a further purification process. Nevertheless, the inert concentrations would rise by removing some ideal assumptions, thus requiring a purification step that, depending on the inert amount, may include flash cascade [8], cryogenic purification [17], or membranes. In order to consistently reproduce the per-formance achieved in the original work, the specific CO_2 com-pression work was assumed equal as in Ref. [8]. The residual stream #27 after carbon capture and storage (CCS) section, mainly containing incondensable species, is simply vented.

Simulation results in terms of energy balances are summarized in Table 2 and show good correspondence to the original calculations.

Some differences arise from the impossibility to reproduce exact part of the ideal heat exchange processes assumed in the original reference, bringing about also minor differences in flow compositions. Moreover, the layout shows some critical assumptions, which will be clarified below when adapting to a second set of assumption reflecting technological constraints on component performances and operating conditions. At any rate, the final results in terms of efficiency are very similar, in both cases showing a stunning net electrical efficiency of about 82% (LHV) with CO_2 capture.

Most of the power output is produced by the SOFC stacks (about 756 MW), while 105 MW are produced by the steam bottoming cycle. The air turbine power is limited to 117 MW, lower than the compression power (150 MW), so that the role of the "gas cycle" is only passive—like for an auxiliary turbocharging system—in the overall energy balances. The high compression power is due to the low polytropic efficiency (0.70) adopted to reproduce the original results in terms of compressor exit temperature [8] and following heat balances. Nevertheless, the difference in the power consumption (12 MW) and in the outlet temperature (389 °C in this work and 398 °C in Ref. [8]) is still significant and may be due to different assumptions related to the intercooler temperature, the number of stages and the pressure ratio subdivision (see Sec. 2.3).

Details about flow compositions are listed in Table 1. It is possible to evidence the high hydrogen composition of the fuel stream entering the SOFC at point #11, with about 63.5% H_2 and 0.5% CO after the shift reactors (aiming to a complete conversion of CO through the shift reaction, in the first reactor, the operating temperature has been set at around 300–350 °C, and for the second at about 200 °C, according to the temperature range of the different catalysts employed in real plants).

It is also possible to appreciate the extremely demanding conditions assumed at the entrance of the exhaust cooler (temperature at 1395 °C on the hot side), which generates the 950-1000 °C streams feeding the HX2 and the reformer (together with the

Table 1 Thermodynamic properties and chemical composition of the relevant streams for the plant in Fig. 1

				Molar fraction (%)								
Point	T (°C)	p (bar)	m (kg/s)	CH_4	C_xH_y	CO	CO_2	H_2	H_2O	Ar	N_2	O_2
1	38.0	30.00	20.53	93.90	4.30	—	1.00	—	—	—	0.80	—
2	615.0	30.00	20.53	93.90	4.30	—	1.00	—	—	—	0.80	—
3	540.1	12.50	20.53	93.90	4.30	—	1.00	—	—	—	0.80	—
4	462.2	12.00	31.96	59.90		0.21	3.77	9.76	25.87	—	0.49	—
5	950.0	12.00	31.96	59.90		0.21	3.77	9.76	25.87	—	0.49	—
6	950.0	11.52	91.96	0.20		11.49	4.76	51.98	31.44	—	0.13	—
7	236.4	11.52	91.96	0.20		11.49	4.76	51.98	31.44	—	0.13	—
8	339.4	10.80	91.96	—		1.80	14.57	62.20	21.30	—	0.13	—
9	232.0	10.80	91.96	—		1.80	14.57	62.20	21.30	—	0.13	—
10	245.4	10.15	91.96	—		0.54	15.85	63.47	20.01	—	0.13	—
11	910.0	10.15	91.96	—		0.54	15.85	63.47	20.01	—	0.13	—
12	964.0	8.80	159.28	—		—	16.39	8.9	74.58	—	0.13	—
13	1395.2	8.70	170.78	—		—	16.35	—	83.29	0.14	0.22	—
14	62.5	8.70	170.78	—		—	16.35	—	83.29	0.14	0.22	—
15	15.0	1.01	337.00	—		—	0.03	—	1.03	0.92	77.29	20.73
16	389.2	10.10	337.00	—		—	0.03	—	1.03	0.92	77.29	20.73
17	910.0	10.10	337.00	—		—	0.03	—	1.03	0.92	77.29	20.73
18	962.0	8.58	269.68	—		—	0.04	—	1.26	1.12	94.26	3.32
19	587.6	1.50	269.68	—		—	0.04	—	1.26	1.12	94.26	3.32
20	15.3	1.50	269.68	—		—	0.04	—	1.26	1.12	94.26	3.32
21	35.0	8.70	170.78	—		—	16.35	—	83.29	0.14	0.22	—
22	25.0	1.50	43.24	—		—	—	—	100.00	—	—	—
23	25.0	100.00	55.06	—		—	100.00	—	—	—	—	—
24	25.0	8.00	71.43	—		—	—	—	100.00	—	—	—
25	550.0	30.00	11.43	—		—	—	—	100.00	—	—	—
26	950.0	12.11	60.00	—		—	—	—	100.00	—	—	—
27	35.0	10.00	1.05	—		—	—	—	23.27	30.03	46.70	—

SOFC cooling stream), both operating at 950 °C at the outlet. Moreover, steam exiting the HRSG shall be also superheated up to 950 °C before entering the reformer. On the other hand, pressure losses on the SOFC are assumed at a rather high value (around 13% at anode and cathode), while SOFC heat losses are limited in the simulation at 1%.

2.3 Cycle Simulation With Updated Assumptions. The second part of the analysis has been focused on simulating a revised power cycle which implements technological constraints related to component operating conditions, although the plant layout is anyway far from usual specifications. More specifically, in order to cope with thermodynamic and technological limits, different modifications with respect to the original layout have been pursued:

- Heat exchangers temperature: the heat exchange network was adapted considering a temperature difference among the streams: either nitrogen removes or supplies heat, a minimum temperature difference with respect to the other flows has been set to 30 °C (former value 0 °C). Details of the heat exchanger thermal balances are reported in the Appendix.
- Heat exchangers pressure: an overall pressure drop of 4% has been assumed for each nitrogen loop: this can be viewed as 2% drop on the heat exchanger where nitrogen releases heat and 2% on each HE where nitrogen removes heat. Consistently, each loop must account for a nitrogen blower which overcomes the pressure losses and sustains the gas circulation; the blower isentropic efficiency has been set to 0.75. In the first case, pressure losses were not considered.
- Steam temperature: maximum steam temperature has been decreased to usual values for steam cycles and consistently set to 550 °C in the HRSG and 600 °C after a dedicated super-heater. This mainly affects the steam provided for the prereforming and the reforming (the latter was 900 °C).
- FC: cell voltage has been decreased to 0.75 V (was 0.96 V). The value was chosen as possible "target" voltage for an SOFC operating at 950–1000 °C, taking into account also the positive effects of pressurization. It must be evidenced that the SOFC works with extremely high air utilization factors ($U_a = 0.83$) to respect the general thermal balance conditions of the first case, so that oxygen fraction at cell outlet is very low.
- FC: in the original analysis, SOFC anode outlet contained for simplicity no carbon monoxide, despite water gas shift reaction does not completely convert the entering CO. Provided that the equilibrium condition out of the SOFC anode is a widely recognized operating condition [30–32], the composition has been recalculated accounting for CO in the products.
- Compressor: the intercooled compression (IC) has been simulated with a polytropic efficiency in line with the state-of-the-art for large axial turbomachinery ($\eta_{poly} = 0.89$ versus 0.7 in the first calculation), in this case with a positive effect on the plant energy balances; minimum temperature after intercooling is set to 35 °C.

Table 2 Power balance for the plant of Fig. 1

Plant of Fig. 1 (original assumptions)	Original Ref. [8]	Calculated	Diff.
Power production	(MW)	(MW)	(MW)
SOFC ($V_c = 0.96$ V)	751.7	756.1	4.40
Steam turbine	97.8	104.57	6.77
Natural gas expander	5.4	5.97	0.57
Cathode exhaust expander	122.8	116.7	−6.10
Consumptions	(MW)	(MW)	(MW)
Air IC compressor	−137.9	−149.78	−11.88
ASU	−13.9	−12.47	1.43
HRSG aux.	−1.5	−2.25	−0.75
CO_2 recovery	−9.5	−9.02	0.48
Overall energy balances	(MW)	(MW)	(MW)
Net power production	815	809.8	−5.20
Fuel inlet	995.38	981.70	−13.68
Net electrical efficiency (LHV) (%)	81.88%	82.49%	0.61%
Net electrical efficiency (HHV) (%)	73.90%	74.45%	0.55%

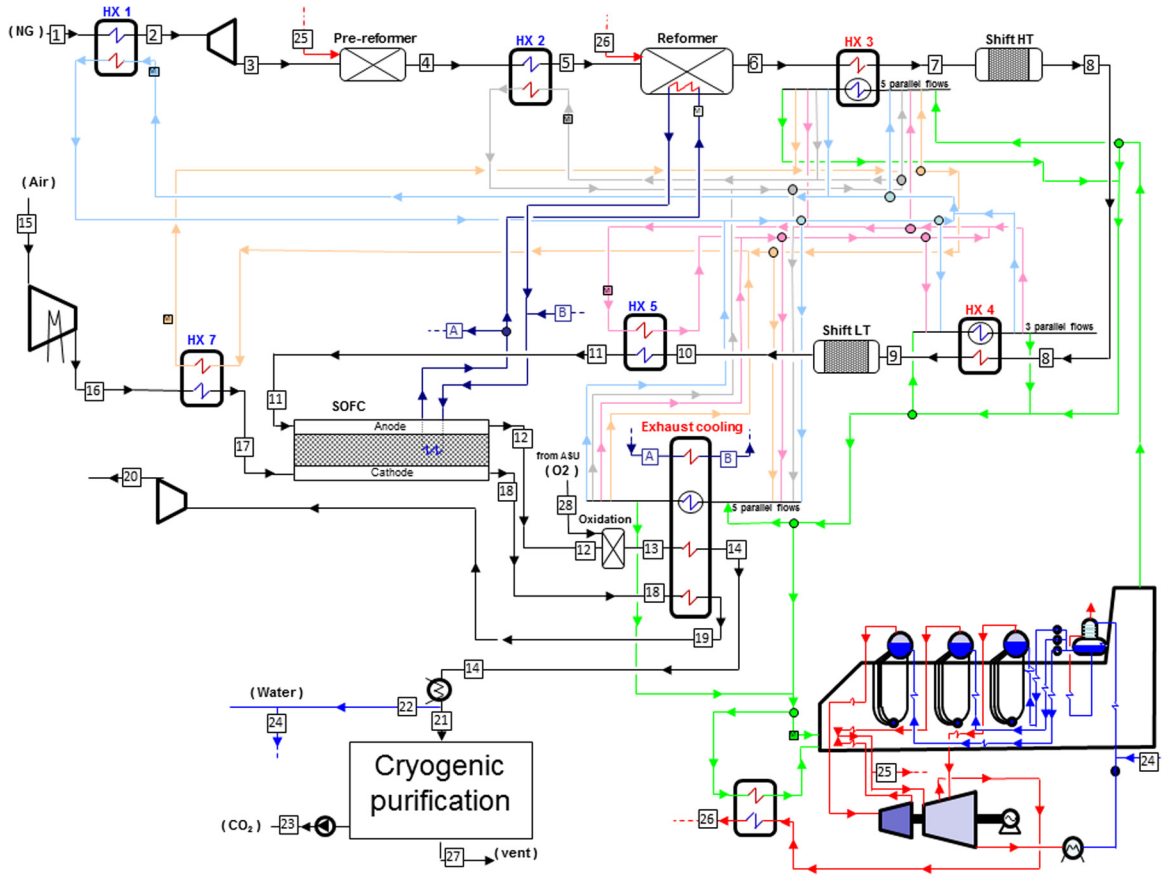

Fig. 2 Plant layout for the simulation with revised assumptions. Details about the flow arrangement as in Fig. 1.

Table 3 Main assumptions for plant simulation (Fig. 2)

Fuel cell		Natural gas and ambient conditions	
Cell voltage	0.75 V	Natural gas composition, molar %	CH_4 93.9, C_2H_6 3.2, C_3H_8 0.7, CO_2 1.0, S 5 ppm
Fuel utilization factor U_f	86%	Natural gas HHV/LHV	52.981/47.818 MJ/kg
Air utilization factor U_a	83%	Ambient conditions	15 °C/1.013 bar/60% RH
Overall[a] $\Delta p/p$ anode/cathode streams	13%		
Heat losses (% inlet thermal power)	1%		
DC–AC converter efficiency	97%		
Air compressor and turbine		**Cryogenic purification and compression**	
Pressure loss at inlet	1 kPa	Final delivery pressure	110 bar
Compressor efficiency η_{poly}	0.89	Compressor isentropic Efficiency	82%
Temperature at the intercooler outlet	35 °C	Pump efficiency	75%
Number of intercooler	1	CO_2 purity	>96%
Turbine η_{poly} (cooled/uncooled stages)	0.89/0.925		
Turbine organic efficiency	0.987		
Generator mechanical/electrical efficiency	0.996/0.985		
Steam cycle			
Pressure levels, bar		130, 30, 7.5 bar	
Maximum temperature HRSG		550 °C	
Pinch, subcooling, approach ΔT		10/5/25 °C	
Condensing pressure		0.048 bar (32 °C)	
Turbine isentropic efficiency		92%/94%/88% (high pressure (HP)/intermediate pressure (IP)/low pressure (LP))	
Pumps efficiency		70%	
HRSG/heat exchangers therm. losses		0.7% of thermal input	
HRSG pressure losses		4 kPa	
Generator/mechanical efficiency		98.5%/99.6%	
Power consumed for heat rejection		0.8% of heat released	

[a]The overall pressure loss is divided between two SOFCs modules with intermediate cooling.

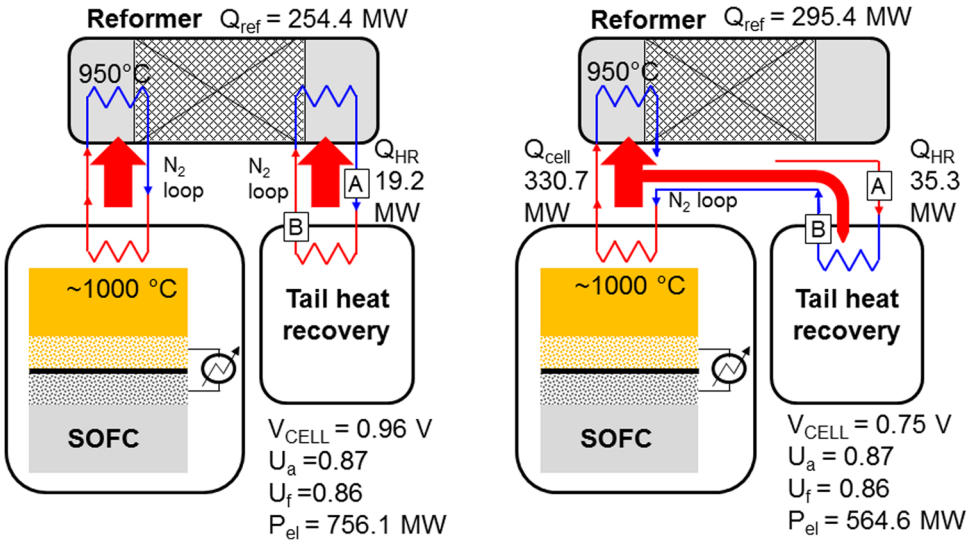

Fig. 3 Thermal integration of the SOFC with the reformer and the tail heat recovery: on the left, the ideal case where the SOFC does not provide all the required heat to the reformer. On the right, the closer to reality case: the lower cell voltage increases the heat production.

- Turbine: the turbine expanding the SOFC cathode exhaust has been moved downstream the multiflow heat exchanger instead of upstream. Although, in principle, a higher tempera-ture turbine, placed ahead the heat exchanger, would allow increasing its operating temperature, this solution was not applicable here: the outlet gas temperature would have become too low to fulfill the thermal balances and to preserve the temperature difference among the hot/cold fluids within the heat exchanger network.
- Reforming heat integration: provided that the heat available increases sharply when the SOFC voltage is lowered, the heat recovery from the stack cooling is larger than the reformer needs. This changes the scope of the stream A–B derived from the SOFC cooling: in the original case it received heat from the cell exhaust and provided energy to the reformer. In the updated case, the SOFC cooling covers the reformer requirements and provides heat also to the HRSG (see also Fig. 3 in the following discussion).
- Oxy-combustion: the oxygen supplied to the anode exhaust combustion has been set to obtain in the flue gas an O_2 molar concentration of 2.5% [33] (previously set to 0%). This value reproduces a realistic oxy-combustion process where a small excess of additional oxygen is required to obtain a complete combustion process. It entails a higher ASU consumption due to the larger required oxygen flow rate.
- CO_2 purification step: as a result of the additional oxygen supplied to the oxy-combustion, the CO_2 rich stream is diluted with inerts, namely, O_2, Ar, and N_2 and must be puri-fied before the storage. Accordingly, a cryogenic separation process has been adopted as described in Ref. [22]. The final delivery purity and pressure has been set to fulfill the sug-gested values reported [28]. The residual stream #27 from the CCS section is vented, this time including excess oxygen which was not present in the first case (where combustion worked at stoichiometric conditions).

The resulting plant layout is shown in Fig. 2, while all the re-vised assumptions discussed above are summarized in Table 3. The corresponding simulation results, in terms of mass balances and thermodynamic conditions, are shown in Table 4.

Results show a remarkable change in cycle performances and power balances (Table 5). Mainly due to the heavy decrease of cell power output (−192 MW) and to the appearance of high energy consumptions in the blowers (+42 MW) which are driving the circulation of N_2 in the network of high temperature heat exchangers, the net electric efficiency drops to 62.7%. Although this remains a pretty high value, it is significantly lower than the efficiency achieved by the "ideal" cycle, and it is obtained with a very complex power plant layout, exploiting a cumbersome heat exchanger network which needs to operate in several cases at high temperatures.

The FC generates about 70% of the gross power output, while the steam turbine 19%, the cathode exhaust expander 10% and the natural gas expander[3] the remaining 1%.

The heat integration comparison between the first and the sec-ond case is depicted in Fig. 3; with a lower cell voltage the heat produced within the cell exceed the reforming needs and is partly used for the tail heat recovery.

The positive power output of the cathode expander is more than counterbalanced by the heavy consumption of the air compressor, requiring 30% more power (103 MW) and driven by a separated electric motor. By this point of view, the power cycle does not exploit the integration with a real "gas turbine" since there is no positive power output from the turbomachinery on the gas loop, so that the only advantage of pressurized operation within this plant configuration would be related to the increase of the SOFC voltage allowed by thermodynamics.

On the other hand, the steam cycle plays a relevant role: to-gether with the air turbine, it basically recovers useful energy from the output streams of a topping system which includes the SOFC + reformer (where fuel input is 981.7 MW) and the air IC compressor (103.4 MW), totalizing a total input of 1085 MW plus the input related to oxygen provided by the ASU.

Aiming to better evidence the power balances in the heat exchanger network of Fig. 2, the Appendix reports a list of the operating conditions in all the main heat exchangers and chemical reactors, in terms of thermal power, mass flow rate, and tempera-ture variation of all the involved streams. Table 6 is related to the heat exchangers operating with two flows, including the reformer. Moreover, several heat exchangers adopt a multiflow configura-tion, and Table 7 shows the situation of all the corresponding hot and cold streams.

Generally speaking, the situation is extremely demanding in terms of maximum material temperatures, heat duties, and required mass flow rates for the stipulated heat transfer fluid (N_2).

[3]This component, recovering energy from the expansion of natural gas taken from high pressure pipelines, is sometimes considered in plant efficiency analysis. His elimination would entail a 0.5% reduction of efficiency.

Table 4 Thermodynamic properties and chemical composition of the relevant streams for the plant of Fig. 2

	T	p	G	Composition, mol. %								
Point	°C	bar	kg/s	CH_4	C_xH_y	CO	CO_2	H_2	H_2O	Ar	N_2	O_2
1	38.0	30.00	20.53	93.90	4.30	—	1.00	—	—	—	0.80	—
2	560.0	29.55	20.53	93.90	4.30	—	1.00	—	—	—	0.80	—
3	481.3	12.50	20.53	93.90	4.30	—	1.00	—	—	—	0.80	—
4	436.1	12.00	31.96	61.07	—	0.12	3.38	7.84	34.75	—	0.49	—
5	890.0	11.82	31.96	61.07	—	0.12	3.38	7.84	34.75	—	0.49	—
6	890.0	11.35	91.96	0.52	—	10.76	5.28	51.86	31.46	—	0.13	—
7	283.5	11.18	91.96	0.52	—	10.76	5.28	51.86	31.46	—	0.13	—
8	355.1	10.73	91.96	—	—	2.10	14.28	61.91	21.58	—	0.13	—
9	232.0	10.57	91.96	—	—	2.10	14.28	61.91	21.58	—	0.13	—
10	248.6	10.15	91.96	—	—	0.56	15.82	63.45	20.04	—	0.13	—
11	850.0	9.99	91.96	—	—	0.56	15.82	63.45	20.04	—	0.13	—
12	950.0	8.70	156.31	—	—	2.43	13.95	8.90	74.59	—	0.13	—
13	1487.1	8.69	177.61	—	—	—	15.91	—	81.05	0.25	0.29	2.50
14	65.5	8.43	177.61	—	—	—	15.91	—	81.05	0.25	0.29	2.50
15	15.0	1.01	337.00	—	—	—	0.03	—	1.03	0.92	77.28	20.73
16	294.6	10.25	337.00	—	—	—	0.03	—	1.03	0.92	77.28	20.73
17	890.0	10.10	337.00	—	—	—	0.03	—	1.03	0.92	77.28	20.73
18	962.0	8.80	272.65	—	—	—	0.04	—	1.25	1.11	93.36	4.25
19	430.1	8.67	272.65	—	—	—	0.04	—	1.25	1.11	93.36	4.25
20	140.7	1.10	272.65	—	—	—	0.04	—	1.25	1.11	93.36	4.25
21	35.0	8.30	62.96	—	—	—	83.38	—	0.68	1.32	1.52	13.10
22	35.0	8.30	114.65	—	—	—	—	—	100.00	—	—	—
23	25.0	110.00	59.81	—	—	—	97.35	—	—	0.35	0.24	2.06
24	20.0	1.01	71.43	—	—	—	—	—	100.00	—	—	—
25	550.0	30.00	11.43	—	—	—	—	—	100.00	—	—	—
26	600.0	12.12	60.00	—	—	—	—	—	100.00	—	—	—
27	35.0	26.00	3.15	—	—	—	28.72	—	—	5.37	6.85	59.05
28	200.0	8.69	21.30	—	—	—	—	—	—	2.00	3.00	95.00

We must recall that nitrogen has been selected here for simplicity as a general-purpose heat transfer fluid for all the heat exchanger network, due to the wide range of temperatures in the complex heat transfer arrangement foreseen by the plant layout. No attempt has been made to optimize the choice, for instance, selecting different fluids for each heat transfer loop, and we did not consider to study the actual heat exchange coefficients and heat transfer surface requirement. However, the results in terms of mass flow rates and heat duty clearly suggest the necessity of a huge heat exchanger equipment. The worst case is the stream transferring heat from the SOFC to the reformer, due also to the relatively small temperature differences featured by its arrangement: it requires to convey 2066 kg/s (as a rule of thumb, three times the air mass flow rate at the compressor of the largest industrial gas turbines on the market) to release 295 MW once cooled from 920 to 800 °C to sustain the reforming reactions.

Table 5 Energy balances of the power cycle in Fig. 2 (plant with updated assumptions)

Power production	(MW)
SOFC	564.6
Steam turbine	155.7
Natural gas expander	5.9
Cathode exhaust expander	80.4
Consumptions	(MW)
Air IC compressor	103.4
ASU	23.1
HRSG aux.	3.0
Nitrogen blowers	41.5
CO_2 recovery and purification	12.5
Water pump	7.4
Overall energy balance	(MW)
Net power production	615.7
Fuel inlet (LHV)	981.7
Net electric efficiency (LHV)	62.7

Several other heat exchangers show a complex multiple-flow arrangement, as evidenced by the example of Fig. 4, and exceed a hundred MW duty, always requiring very large mass flow rates of the heat transfer fluid. In addition, in several heat exchangers, the wall materials should be developed to face a very high temperature (around 900 °C in the worst cases).

By this point of view, these preliminary results evidence that the plant layout would require further evolution to get closer to an engineering feasibility. On the other hand, the analysis also confirms the better perspectives of different power plant solutions discussed in literature, which exploit internal reforming within the FC (with no separated heat transfer loops as those required by the power plant considered here) to simplify the plant heat management, both for applications without CO_2 capture [9,10] and for CCS [3,4,11,12].

3 Conclusions

This work presented the thermodynamic analysis of an SOFC power cycle applied to electricity generation with CO_2 capture, based on a prereforming concept where fuel is reformed ahead the SOFC, operated with a high hydrogen content fuel.

Following a literature review on very promising plant configurations, the reference plant is selected and first reproduced considering all the assumptions proposes by the original authors, which in some cases refer to ideal operating conditions. The calculated performance is extremely high, confirming the original results with about 82% LHV electrical efficiency in ideal operating con-ditions and full CO_2 capture, making it an interesting plant config-uration. As a second step, the simulations were focused on updating the power cycle, implementing a complete set of assumptions about component losses and technological constraints on component performances. The new simulation included more conservative operating conditions about FC voltage, heat exchangers minimum temperature differences, maximum steam temperature, turbomachinery efficiency, component pressure losses, and other adjustments. Following the consequent

modifications with respect to the original layout, it turns out the necessity of including a bulky heat exchanger network, extremely demanding in terms of high wall temperatures, large heat duties, and required mass flow rates. The power contribute of the gas turbine cycle is globally negative (compressor duty is higher than expander power), so that the only advantage of pressurized operation within this plant configuration is related to the increase of SOFC voltage allowed by thermodynamics. The net electric efficiency changes to around 63% LHV with nearly complete (95%+) CO_2 capture, a still remarkable but less attractive value given the plant complexity.

By this point of view, the analysis also confirms the better perspectives of different power plant solutions discussed in literature, which exploit internal reforming within the FC (with no separated heat transfer loops) to simplify the plant heat management.

Nomenclature

ASU = air separation unit
FC = fuel cell
HHV = higher heating value (MJ/kg)
HRSG = heat recovery steam generator
HTS = high temperature shift
LHV = lower heating value (MJ/kg)
LTS = low temperature shift
m = mass flow rate (kg/s)
MTS = medium temperature shift
p = total pressure (bar)
P = power (MW)
SOFC = solid oxide fuel cell
T = temperature (°C or K)
U_a = air utilization factor: $U_a = O_{2,consumed}/O_{2,inlet}$
V = fuel cell potential (V)

Subscripts

a = air
e = electric
f = fuel
in = inlet
reac = reaction
Th = thermal

Appendix

The overall heat exchange network is reported in Tables 6 and 7 and Fig. 4. Heat removal from the SOFC has been modeled splitting the SOFC in two modules, with intermediate and final

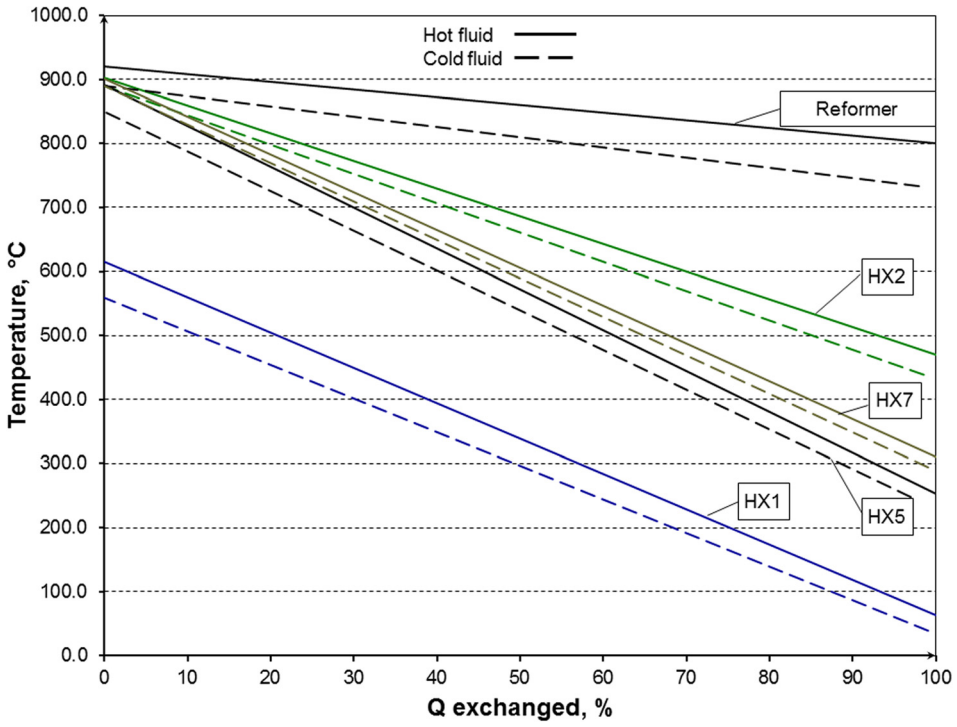

Fig. 4 Temperature heat exchanged diagram for the heat exchangers reported in Table. 6

Table 6 Thermal balances of heat exchangers providing heat to the fuel/syngas before the SOFC stack according to the layout proposed in Fig. 2

	Stream	Duty (MW)	Type	Mass flow (kg/s)	T_{in} (°C)	T_{out} (°C)	Heat loss (MW)
HX1	Cold flow	−32.50	Fuel	20.5	38.0	560.0	−0.33
	Hot flow	32.83	Nitrogen	55.0	614.5	63.0	
HX 2	Cold flow	−50.36	Fuel	31.96	436.1	890.0	−0.51
	Hot flow	50.87	Nitrogen	100.95	903.2	470.1	
Reformer	Cold flow	−289.45	Fuel	91.96	733.7	890.0	−5.90
	Hot flow	295.36	Nitrogen	2066.0	920.0	800.0	
HX 5	Cold flow	−161.05	Fuel	91.96	248.6	850.0	−5.03
	Hot flow	166.03	Nitrogen	230.2	890.8	253.1	
HX 7	Cold flow	−224.25	Air	337.0	393.1	890.0	−1.91
	Hot flow	226.52	Nitrogen	336.65	900.9	310.0	

Table 7 Thermal balances of heat exchangers operating with multiple flows within the plant of Fig. 2

	Stream	Duty (MW)	Type	Mass flow (kg/s)	T_{in} (°C)	T_{out} (°C)	Heat loss (MW)
HX 3	Hot flow	158.2	Fuel	92.0	890.0	283.6	−2.2
	Cold flow 1	−2.8	Nitrogen HX 1	4.7	63.0	615.0	
	Cold flow 2	−12.8	Nitrogen HX 2	28.4	470.1	860.0	
	Cold flow 3	−35.4	Nitrogen HX 5	51.6	253.1	860.0	
	Cold flow 4	−37.7	Nitrogen HX 7	60.4	310.0	860.0	
	Cold flow 5	−5.1	Nitrogen HRSG prereforming	8.6	21.0	575.0	
	Cold flow 6	−33.8	Nitrogen HRSG reforming	40.0	88.7	850.0	
	Cold flow 7	−28.5	Nitrogen HRSG bottom	49.7	43.0	575.0	
HX 4	Hot flow	31.2	Fuel	92.0	355.1	232.0	−0.5
	Cold flow 1	0.0	Nitrogen HX 1	0.1	63.0	340.0	
	Cold flow 2	0.0	Nitrogen HX 5	0.1	253.1	340.0	
	Cold flow 3	−30.7	Nitrogen HRSG prereforming	91.3	21.0	340.0	
	Cold flow 4	0.0	Nitrogen HRSG reforming	0.1	88.7	340.0	
	Cold flow 5	0.0	Nitrogen HRSG bottom	0.1	43.0	340.0	
SOFC cooler 1	Hot flow 1	55.3	Anode gas	123.2	1125.8	950.0	−1.80
	Hot flow 2	64.7	Cathode gas	305.7	1125.8	950.0	
	Cold flow 1	−118.2	Nitrogen from reformer	826.5	800.0	920.0	
SOFC cooler 2	Hot flow 1	124.5	Anode gas	159.3	1300.6	950.0	−3.5
	Hot flow 2	112.0	Cathode gas	269.7	1300.6	962.0	
	Cold flow 1	−232.9	Nitrogen from reformer	1629.3	800.0	920.0	
Anode ex.cooler 1	Hot flow	153.9	Anode exhaust	170.8	1395.1	980.0	−2.3
	Cold flow 1	−5.2	Nitrogen HX 2	10.0	470.1	920.0	
	Cold flow 2	−33.2	Nitrogen HX 5	45.4	253.1	900.0	
	Cold flow 3	−52.8	Nitrogen HX 7	77.2	310.0	910.0	
	Cold flow 4	−60.4	Nitrogen HRSG reforming	71.4	88.7	850.0	
Anode ex.cooler 2	Hot flow 1	552.4	Anode exhaust	170.8	980.0	70.0	−9.14
	Hot flow 2	55.7	Nitrogen from SOFC cooling (A–B)	389.8	920.0	800.0	
	Cold flow 1	−20.1	Nitrogen HX 1	33.7	63.0	615.0	
	Cold flow 2	−20.3	Nitrogen HX 2	39.0	470.1	920.0	
	Cold flow 3	−86.3	Nitrogen HX 5	117.9	253.1	900.0	
	Cold flow 4	−122.8	Nitrogen HX 7	179.6	310.0	910.0	
	Cold flow 5	−15.3	Nitrogen HRSG prereforming	25.6	21.0	575.0	
	Cold flow 6	−184.4	Nitrogen HRSG reforming	218.2	88.7	850.0	
	Cold flow 7	−149.7	Nitrogen HRSG bottom	275.1	43.0	550.0	
Cathode ex. cooler	Hot flow	167.2	Cathode exhaust	269.7	962.0	424.4	−2.3
	Cold flow 1	−9.9	Nitrogen HX 1	16.5	63.0	615.0	
	Cold flow 2	−12.6	Nitrogen HX 2	24.1	470.1	920.0	
	Cold flow 3	−11.1	Nitrogen HX 5	15.2	253.1	900.0	
	Cold flow 4	−13.2	Nitrogen HX 7	19.4	310.0	910.0	
	Cold flow 5	−14.3	Nitrogen HRSG prereforming	24.0	21.0	575.0	
	Cold flow 6	−32.2	Nitrogen HRSG reforming	38.1	88.7	850.0	
	Cold flow 7	−71.6	Nitrogen HRSG bottom	125.0	43.0	575.0	

cooling (the corresponding heat exchangers are listed as SOFC coolers). Several heat exchangers adopt a multiflow configuration; Table 7 shows the situation of all the corresponding hot and cold streams.

References

[1] Hirschenhofer, J. H., Staffer, D. B., and White, J. S., 1994, "Carbon Dioxide Capture in Fuel Cell Power Systems," International Energy Conversion Engineering Conference, New York, Monterey, CA, AIAA Paper No. 94-4148-CP, pp. 1120–1125.

[2] Wolsky, A. M., Daniels, E. J., and Jody, B. J., 1993, "Technologies for CO_2 Capture From Advanced Power-Generation Systems," Energy Systems Division, Argonne National Laboratory, Argonne, IL, Report No. ANL/ES/CP–80346, available at: http://www.osti.gov/scitech/servlets/purl/10177996

[3] Campanari, S., and Chiesa, P., 2000, "Potential of Solid Oxide Fuel Cells (SOFC) Based Cycles in Low-CO_2 Emission Power Generation," 5th International Conference on Greenhouse Gas Control Technologies (GHGT-5), Cairns, Australia, Aug. 13–16.

[4] Campanari, S., 2002, "Carbon Dioxide Separation From High Temperature Fuel Cell Power Plants," J. Power Sources, **112**(1), pp. 273–289.

[5] Akai, M., Nomuna, N., Waku, H., and Inoue, M., 1997, "Life-Cycle Analysis of a Fossil-Fuel Power Plant With CO_2 Recovery and a Sequestering System," Energy, **22**(2–3), pp. 249–255.

[6] Damen, K., Van Troost, M., Faaij, A., and Turkenburg, W., 2006, "A Comparison of Electricity and Hydrogen Production Systems With CO_2 Capture and Storage. Part A: Review and Selection of Promising Conversion and Capture Technologies," Prog. Energy Combust. Sci., **32**(2), pp. 215–246.

[7] Liese, E., 2009, "Comparison of Pre-Anode and Post-Anode Carbon Dioxide Separation for IGFC Systems," ASME Paper No. GT2009-59144.

[8] Adams, T. A., and Barton, P. I., 2010, "High-Efficiency Power Production From Natural Gas With Carbon Capture," J. Power Sources, **195**(7), pp. 1971–1983.

[9] Litzinger, K. P., Veyo, S. E., Shockling, L. A., and Lundberg, W. L., 2005, "Comparative Evaluation of SOFC/Gas Turbine Hybrid System Options," ASME Paper No. GT2005-68909.

[10] Trasino, F., Bozzolo, M., Magistri, L., and Massardo, A. F., 2009, "Modelling and Performance Analysis of the Rolls-Royce Fuel Cell System Limited 1 MW Plant," ASME Paper No. GT2009-59328.

[11] Tsuji, T., Yanai, N., Fujii, K., Miyamoto, H., Watabe, M., Ishiguro, T., Ohtani, Y., and Uechi, H., 2003, "Multi-Stage Solid Oxide Fuel Cell–Gas Turbine Combined Cycle Hybrid Power Plant System," ASME Paper No. GT2003-38391.

[12] Moller, B. F., Arriagada, J., Assadi, M., and Potts, I., 2004, "Optimisation of an SOFC/GT System With CO_2-Capture," J. Power Sources, **131**(1–2), pp. 320–326.

[13] Vivanpatarakij, S., Laosiripojana, N., Kiatkittipong, W., Arpornwichanop, A., Soottitantawat, A., and Assabumrungrat, S., 2009, "Simulation of Solid Oxide Fuel Cell Systems Integrated With Sequential CaO–CO_2 Capture Unit," Chem. Eng. J., **147**(2–3), pp. 336–341.

[14] Piroonlerkgul, P., Laosiripojana, N., Adesina, A. A., and Assabumrungrat, S., 2009, "Performance of Biogas-Fed Solid Oxide Fuel Cell Systems Integrated With Membrane Module for CO_2 Removal," Chem. Eng. Process., **48**(2), pp. 672–682.

[15] Carson, J. L., 1995, "Thermodynamics of Pressure Swing Adsorption (PSA) in the Recovery of Residual Hydrogen From SOFC Anode Gas," Intersociety

Energy Conversation Engineering Conference, Orlando, FL, July 30–Aug. 4, pp. 229–234.
[16] Duan, L., Yang, Y., He, B., and Xu, G., 2012, "Study on a Novel Solid Oxide Fuel Cell/Gas Turbine Hybrid Cycle System With CO_2 Capture," Int. J. Energy Res., **36**(2), pp. 139–152.
[17] Campanari, S., Chiesa, P., and Manzolini, G., 2009, "CO_2 Capture From Combined Cycles Integrated With Molten Carbonate Fuel Cells," Int. J. Greenhouse Gas Control, **4**(3), pp. 441–451.
[18] Kuramochi, T., Turkenburg, W., and Faaij, A., 2011, "Competitiveness of CO_2 Capture From an Industrial Solid Oxide Fuel Cell Combined Heat and Power System in the Early Stage of Market Introduction," Fuel, **90**(3), pp. 958–973.
[19] Jericha, H., Hacker, V., Sanz, W., and Zotter, G., 2010, "Thermal Steam Power Plant Fired by Hydrogen and Oxygen in Stoichiometric Ratio, Using Fuel Cells and Gas Turbine Cycle Components," ASME Paper No. GT2010-22282.
[20] Park, S. K., Kim, T. S., Sohn, J. L., and Lee, Y. D., 2011, "An Integrated Power Generation System Combining Solid Oxide Fuel Cell and Oxy-Fuel Combustion for High Performance and CO_2 Capture," Appl. Energy, **88**(4), pp. 1187–1196.
[21] Riensche, E., Achenbach, E., Froning, D., Haines, M. R., Heidug, W. K., Lokurlu, A., and Von Andrian, S., 2000, "Clean Combined-Cycle SOFC Power Plant—Cell Modelling and Process Analysis," J. Power Sources, **86**(1–2), pp. 404–410.
[22] Chiesa, P., Campanari, S., and Manzolini, G., 2011, "CO_2 Cryogenic Separation From Combined Cycles Integrated With Molten Carbonate Fuel Cells," Int. J. Hydrogen Energy, **36**(16), pp. 10355–10365.
[23] Consonni, S., Lozza, G., Macchi, E., Chiesa, P., and Bombarda, P., 1991, "Gas-Turbine-Based Advanced Cycles for Power Generation Part A: Calculation Model," International Gas Turbine Conference, Yokohama, Japan, Oct. 27–Nov. 1, Vol. III, pp. 201–210.
[24] Lozza, G., 1990, "Bottoming Steam Cycles for Combined Gas Steam Power Plants: A Theoretical Estimation of Steam Turbine Performance and Cycle Analysis," ASME Cogen Turbo, New Orleans, LA, Aug. 27–29, pp. 83–92.
[25] Chiesa, P., Consonni, S., Kreutz, T., and Williams, R., 2005, "Co-Production of Hydrogen, Electricity and CO_2 From Coal With Commercially Ready Technology. Part A: Performance and Emissions," Int. J. Hydrogen Energy, **30**(7), pp. 747–767.
[26] Campanari, S., and Macchi, E., 1998, "Thermodynamic Analysis of Advanced Power Cycles Based Upon Solid Oxide Fuel Cells, Gas Turbines and Rankine Bottoming Cycles," ASME Paper No. 98-GT-585.
[27] Campanari, S., Iora, P., Macchi, E., and Silva, P., 2007, "Thermodynamic Analysis of Integrated MCFC/Gas Turbine Cycles for Multi-MW Scale Power Generation," ASME J. Fuel Cell Sci. Technol., **4**(3), pp. 308–316.
[28] Franco, F., Anantharaman, R., Bolland, O., Booth, N., Dorst, E. V., and Ekstrom, C., 2011, "European Best Practice Guide for Assessment of CO_2 Capture Technologies," European Benchmarking Task Force (EBTF), Report No. 213206, available at: http://www.energia.polimi.it/news/D%204_9%20best%20practice%20guide.pdf
[29] Manzolini, G., Macchi, E., Binotti, M., and Gazzani, M., 2011, "Integration of SEWGS for Carbon Capture in Natural Gas Combined Cycle. Part B: Reference Case Comparison," Int. J. Greenhouse Gas Control, **5**(2), pp. 214–225.
[30] Campanari, S., and Iora, P., 2005, "Comparison of Finite Volume SOFC Models for the Simulation of a Planar Cell Geometry," Fuel Cells, **5**(1), pp. 34–51.
[31] Aguiar, P., Adjiman, C. S., and Brandon, N. P., 2004, "Anode-Supported Interme-diate Temperature Direct Internal Reforming Solid Oxide Fuel Cell. I: Model-Based Steady-State Performance," J. Power Sources, **138**(1–2), pp. 120–136.
[32] Iwai, H., Yamamoto, Y., Saito, M., and Yoshida, H., 2011, "Numerical Simulation of Intermediate-Temperature Direct-Internal-Reforming Planar Solid Oxide Fuel Cell," Energy, **36**(4), pp. 2225–2234.
[33] Romano, M., 2013, "Ultra-High CO_2 Capture Efficiency in CFB Oxyfuel Power Plants by Calcium Looping Process for CO_2 Recovery From Purification Units Vent Gas," Int. J. Greenhouse Gas Control, **18**, pp. 57–67.